Maximising Network Capacity with Service Provisioning in QKD-Integrated Optical Networks

Yuhang Liu
State Key Lab of Information Photonics and Optical Communications, Beijing University of Posts and Telecommunications
Beijing, 100876 China
yuhangliu@bupt.edu.cn

Xiaosong Yu
State Key Lab of Information Photonics and Optical Communications, Beijing University of Posts and Telecommunications
Beijing, 100876 China
xiaosongyu@bupt.edu.cn

Yongli Zhao
State Key Lab of Information Photonics and Optical Communications, Beijing University of Posts and Telecommunications
Beijing, 100876 China
yonglizhao@bupt.edu.cn

***Abstract*—Quantum communication is envisioned as a foundational technology for future secure communication. Owing to the stable transmission properties of optical fibre, quantum communication is likely to be implemented over fibre infrastructures, currently with quantum key distribution (QKD) being the most representative protocol for deployment. The optical infrastructure is dominated by data services, where limited network resources are allocated for service provisioning. To cost-effectively scale QKD services to support multi-point users' secured communication, it remains a critical challenge to share the existing optical networks' capacity without disrupting legacy data services. At the same time, the variant distribution of data traffic leads to dynamic interference on the traversed QKD systems. In this paper, we focus on the QKD-integrated optical networks scenario, and investigate the network capacity maximization solutions. The network resources are shared by QKD and data services, where quadratic programming is utilised to optimise the service provisioning while minimising its interference on traversed quantum channels. Simulation results demonstrate that the outcome solution increases the average secret key rate in a 9-node mesh network from 0.38 Mbit/s to 6.51 Mbit/s, comparing with the first-fit benchmark. This outcome is achieved without blocking any data service request.**

Keywords—Quantum key distribution, optical network, service provisioning, network capacity

I. INTRODUCTION

Based on the principles of quantum physics, quantum communication is considered a promising paradigm for future trustworthy networks. Due to technical challenges such as quantum memory limitations, the development of quantum networks is still in early stages [1]. In this context, quantum key distribution (QKD), which integrates qubit transmission with classical post-processing, has become the most practically realisable quantum communication protocol to date. With the strict limitation of the quantum-physics principle, each data-encryption user must be associated with a QKD node that resides within the same physical trusted domain, ensuring secure key delivery [2], [3]. This highlights the need to build a quantum communication infrastructure capable of supporting QKD applications, as well as for future quantum applications. Given the stability of optical fibres for qubit transmission, many countries have launched QKD networks over fibre infrastructure as an initial stage of quantum networks, which shows significant deployment cost. As an alternative to building dedicated infrastructure, integrating QKD into existing telecommunication networks has emerged as a more cost-effective and scalable solution [4].

To integrate QKD into the existing optical networks, the quantum channel (QCh) is multiplexed with data channels (DChs), which is considered the first step. However, the high-power DChs cause severe interference to the QCh [5]. The existing wavelength assignment approaches can be divided into two categories: single-band and multi-band deployment. This distinction stems from the fact that the wavelength separation is the main variation on the strength of the interference, especially for the dominant spontaneous Raman scattering (SpRS). Among the multi-band deployment, O+C band is a mainstream approach [6]. While this approach well mitigates SpRS, it introduces compatibility issues with current optical infrastructures, where most optical components support C-band operations [6]. At the same time, assigning QCh to the O-band imposes higher optical loss to the quantum signals, limiting maximum transmission distance to approximately 80 km [6]. Recently, C-band-based coexistence of QCh and DCh is considered an essential candidate against the above limitations [7]. This causes more severe and uncontrolled SpRS. At the same time, the allocation of QCh could interfere with the wavelength continuity for routing of classical data services.

In this work, we analyse the network behavior under the C-band coexistence scenario of QKD and classical data services. As optical networks are becoming flexible in service provisioning, apart from several existing solutions [8], [9], [10], we identify a new perspective for improving the optical network capacity with the integration of QKD. The QKD service is assumed to be operated in an off-line manner, where QKD key generation and session key delivery are separately operated. Considering the dynamic variation of service requests and associated DChs allocation, the interference is not always strongly imposed on the QCh. In this context, with limited network resource, how to maximize the capacity for service provisioning of both data traffic and key generation becomes a network optimisation problem. We thus derive a quadratic programming (QP) model to obtain the solution under the joint constraints imposed by the coexistence of QKD and data services, where we define quantum-classical network capacity as the optimisation objective. The first-fit service provisioning approach is set as the benchmark. Considering the computational complexity of optical network provisioning, which is known to be NP-hard, we compare the optimisation solutions under varying time constraints for the QP solver. Considering the maturity of discrete-variable QKD (DV-QKD) in metropolitan scenarios, the simulations were conducted in typical metropolitan network topologies, including ring, tree, and mesh topologies. With a fixed set of

service arrivals, an increase in average SKR from 0.38 Mbit/s to 6.51 Mbit/s was observed in the 9-node mesh topology. The optimisation was achieved without blocking any data services.

II. Flexible Service Provisioning for QKD Integration in Optical Transport Networks

To meet the security requirements of session key delivery via QKD, at least one QKD system should be deployed in each data communicating node (DCN) pair. With the QKD integration, the network service provider is capable of provisioning both QKD and classical data services. As shown in Fig. 1, the QKD service provisioning involves configuring both QKD modules (QKDMs) and key managers (KMs), where the QKD keys generated by QKDMs are first synchronized and then stored in the KM. Then, the keys in KMs are relayed using one-time pad encryption to form the end-to-end session keys for data encryption. The key generation is thus operated asynchronously to the data services. The initialisation of QKDM and the configuration of associated QCh are performed once the QKD system is initialised to continuously supply keys for secure storage. In addition to key delivery, each data service provisioning includes the selection of wavelengths. An optical path is then constructed from source node to destination node, subject to the wavelength consistency constraint.

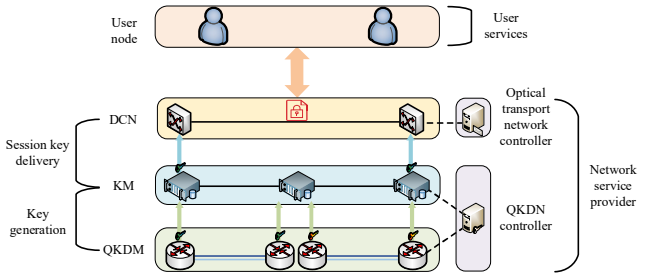

Fig. 1. Illustration of service provisioning in QKD-integrated optical transport networks.

With the coexistence of QKD and data services, the variations in data services and associated DCh configurations dynamically interfere with QChs along traversed links, degrading key generation performance. In a metropolitan network scale, where the fibre length is typically 50 km, the interference is dominated by SpRS [5]. Many studies have investigated solutions to mitigate SpRS, mostly from a system-level perspective [6]. It is observed that in telecom fibre-based QCh–DCh coexistence, the strength of SpRS mainly depends on the wavelength separation and initial power of DChs on each link. This effect can be further amplified at the network scale. For each data service, the optical path imposes SpRS along the traversed QChs, thus dynamically affects the network-wide key generation. With a limited key generation capacity, it could be difficult for KMs to perform the key relay and session key delivery, thus interrupting the QKD service. Therefore, the network service provider has to ensure the connectivity of conventional data services while optimising the distribution of DChs to enhance key generation capacity. This involves dynamically optimise routing, QCh-DCh wavelength separation, and transmission power, posing challenges for network management.

As shown in Fig. 2, with a sequence of user service requests, two kinds of traffic patterns for service provisioning can be formulated in the network. Fig. 2(a) illustrates the aggregated traffic pattern for service provisioning, where request #1 and #2 are allocated with the same routing path. This configuration shows no SpRS impact on optical path A-B-D, but results in higher interference on optical path A-C-D. This could lead to key shortage along the key relay route A-C-D during the time window of requests #1 and #2. However, for the key delivery between node A and D, the key generation along route A-B-D can still supply session keys for encryption services. In this case, this indicates that the aggregated traffic pattern mainly affects the key delivery for encryption services over link A-C and link C-D. In contrast, link A-D can still maintain session keys via route A-B-D.

Figure 2(b) illustrates the distributed traffic pattern for service provisioning, where user requests #1 and #2 are assigned to separate paths: A-B-D and A-C-D. With fewer DChs allocated to A-C-D, SpRS interference is reduced, enabling increased key generation capacity. This leads to a moderate case that both A-B-D and A-C-D suffer from shared SpRS, thus avoiding any key delivery bottlenecks. But according to the strength of SpRS with C-band coexistence, this may reduce the overall network-wide key generation capacity, where the accumulation of session keys from both A-B-D and A-C-D in a time duration may be lower than under the aggregated traffic pattern. Based on the above, there exists a trade-off between traffic distribution and the network-wide QKD capacity, posing an NP-hard constrained optimisation problem. Several works focus on developing a threshold for a specific coexistence scenario, where when the launch power of aggregated DChs over each link exceeds this threshold, the data services can be provisioned using alternative paths to avoid the interruption in the traversed QKD systems [8], [9]. This threshold is usually fixed as a maximum accepted value for non-zero secret key rate of the QKD system. Meanwhile, heuristic algorithms for routing and wavelength assignment are proposed with consideration of quantum interference [10].

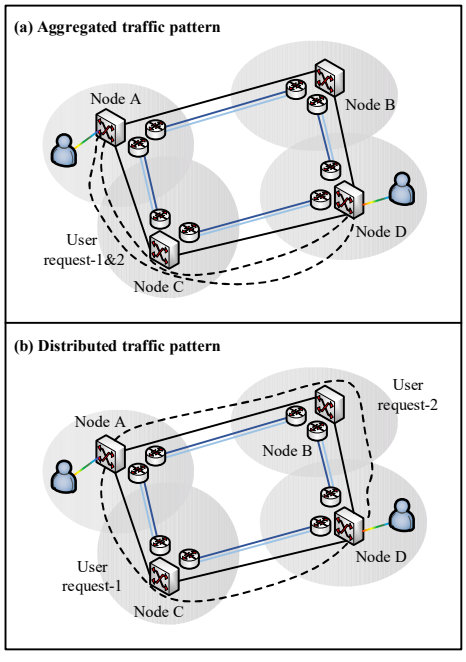

Fig. 2. Comparison of aggregated and distributed traffic patterns in QKD-integrated optical transport networks

In this work, given the unique provisioning pattern of QKD, as well as the dominance of data services in optical transport networks, we allow temporary interruptions of QKD for data service transmission. Since the QKD key generation and session key delivery operate asynchronously, the network service provider is assumed to allow the temporary interruption of key generation when dealing with a heavy traffic load. Thus, without QKD-specific constraints on data service provisioning, balancing traffic distribution and key generation capacity is essential to maximising both data services and QKD services capacity. We analyse the detailed impact model for flexible data service carrying on the secret key rate under dynamic service arrivals, and derive a QP model to capture the trade-off with quantum-classical network capacity as an optimisation objective. We set time limits for the QP solver to get near-optimised solutions and compare it with a conventional first-fit provisioning strategy.

III. Network Formulation and Service Provisioning Optimisation with Quadratic Programming

To determine the maximum network capacity for both data services and key generation, we formulate an integrated model of optical transport networks with QKD. From the perspective of routing and wavelength assignment, we incorporate SpRS and adjacent channel crosstalk effects to characterise the interaction between data services and secret key rate. With this model, we define an optimisation objective under networking constraints to optimise service provisioning.

A. Optical Transport Network Model with QKD Integration

At the arrival of service requests, the optical transport network is formulated as $G = (V, E, \Lambda)$, where V denotes the set of nodes, E denotes the set of edges, Λ denotes the set of wavelength channels. Each data service r involves transmitting data to the destination node through an optical path, which is assumed to be optically transparent, with a DCh assigned along each traversed link following the wavelength consistency constraint. For QKD, a QCh and a measurement-assisted channel (MCh) pair is initiated on each link. In this work, for cost efficiency, each optical link includes only one QKD system, where the MCh is assumed to be time-multiplexed with the DCh. The multi-QKD link configurations are beyond the scope of this work. Thus, the total number of wavelength channels $|\Lambda_e|$ assigned to the QCh $|\Lambda_e^{\mathrm{Q}}|$ and DChs $|\Lambda_{r,e}^{\mathrm{C}}|$ for the traversed services $r \in R$ on an edge e can be expressed as:

$$\sum_{r\in R}|\Lambda_{r,e}^{\mathrm{C}}| + |\Lambda_e^{\mathrm{Q}}| \le |\Lambda_e|, \forall e \in E \tag{1}$$

On each traversed edge (u, v), the active DCh for data service r induces a crosstalk photon count $p_{r,e}$ on the QCh. This includes two major components: the SpRS denoted as $p_{r,(u,v)}^{\mathrm{SpRS}}$, and the adjacent-channel crosstalk, denoted as $p_{r,v}^{\mathrm{AC}}$. The total crosstalk photon count $p_{r,(u,v)}$ can be expressed as:

$$p_{r,(u,v)} = \sum_{v\in V} K_v^r \cdot p_{r,v}^{\mathrm{AC}} + \sum_{(u,v)\in E} K_{(u,v)}^r \cdot p_{r,(u,v)}^{\mathrm{SpRS}} \tag{2}$$

where $p_{r,v}^{\mathrm{AC}}$ denotes the interference experienced at the node v. Meanwhile, $p_{r,(u,v)}^{\mathrm{SpRS}}$ denotes the interference imposed on the QCh over the traversed links. K_v^r and $K_{(u,v)}^r$ are binary indicators of node v and edge (u, v) traversed by service r. As a result, the secret key rate of each edge is affected by the dynamic variation in DCh allocation throughout the services' duration. The Gottesman-Lo-Lütkenhaus-Preskill (GLLP) security framework is adopted for the calculation of secret key rate, denoted as R^{GLLP} [11], which is calculated as:

$$R^{\mathrm{GLLP}} \le (q \cdot (Q_1(1 - h(e_1)) - f Q_\mu h(E_\mu))) \tag{3}$$

$$R_e^{\mathrm{S}} = R^{\mathrm{GLLP}}/T_s \tag{4}$$

where T_s denotes the pulse repetition interval of the DV-QKD system. For (3), Q_1, e_1, Q_μ, and E_μ are formulated as follows:

$$Q_1 = Y_1 \mu e^{-\mu} \tag{5}$$

$$e_1 = (Y_0/2 + e_d\eta)/Y_1 \tag{6}$$

$$Q_\mu = 1 - (1 - Y_0) \cdot \mathrm{e}^{-\eta\mu} \tag{7}$$

$$E_\mu = (Y_0/2 + e_d(1 - \mathrm{e}^{-\eta\mu}))/Q_\mu \tag{8}$$

In the above equations, μ denotes the average number of photons per signal pulse, e_d denotes the phase error probability, η denotes the channel transmittance. Y_0 denotes the vacuum state yield, Y_1 denotes yield of single-photon states. Under the interference introduced by DCh, Y_0 and Y_1 can be further formulated as:

$$Y_0^{(u,v)} = 1 - (1 - (p_{\mathrm{d}} + \textstyle\sum_{r\in R_{(u,v)}} p_{r,(u,v)}))^2 \tag{9}$$

$$Y_1 = Y_0^{(u,v)} + \eta \tag{10}$$

where $Y_0^{(u,v)}$ accounts for the intrinsic dark count probability p_{d}, as well as crosstalk photon counts from active services that share the same edge (u, v). In this context, η is formulated as:

$$\eta = \eta_{\mathrm{d}} \mathrm{e}^{-\alpha L_{(u,v)}} \tag{11}$$

where η_{d} denotes the quantum efficiency of the single-photon detector. α denotes the fibre loss coefficient, and L_e denotes the length of edge (u, v).

B. Quantum-Classical Network Capacity Maximisation

To quantify the network capacity for both data and QKD services, we define an indicator, denoted as the *quantum-classical network capacity* Φ, which is expressed as:

$$\Phi = \alpha \cdot U^{\mathrm{C}} - \delta \cdot I^{\mathrm{CQ}} + \beta \cdot U^{\mathrm{Q}} \tag{12}$$

where U^{C} represents the total number of occupied DChs for data services, U^{Q} denotes the aggregate achievable secret key rate. The term I^{CQ} represents the total interference occurring in all links. α, δ, β are weighting coefficients assigned to each respective term. We use $\widehat{u_r^{\mathrm{C}}}$, $\widehat{u^{\mathrm{Q}}}$, and $\widehat{I_r^{\mathrm{CQ}}}$ to denote the normalised variation of U^{C}, U^{Q}, and I^{CQ} as follows:

$$\widehat{u_r^{\mathrm{C}}} = \frac{\sum_{r\in R} K_{\lambda_n^{\mathrm{C}}}^r}{|R|\cdot|\Lambda_G|} \tag{13}$$

$$\widehat{I_r^{\mathrm{CQ}}} = \sum_{r\in R}\sum_{(u,v)\in E} \frac{K_{\lambda_m^{\mathrm{Q}}}^{(u,v)}}{|\Lambda_e|} \cdot \frac{K_{\lambda_n^{\mathrm{C}}}^r}{|R|\cdot|\Lambda_G|} \cdot p_{r,(u,v)} \tag{14}$$

$$\widehat{u^{\mathrm{Q}}} = \frac{\sum_{e\in E} R_e^{\mathrm{S}}}{|E|} \tag{15}$$

where $K_{\lambda_n^{\mathrm{C}}}^r$ denotes the availability of the wavelength channel λ_n^{C} for DCh of a request r.

Due to the direction-dependent nature of interference between the QCh and DChs, the crosstalk photon count is

categorized into co-propagating and counter-propagating components. $p_{r,v}^{\mathrm{AC}}$ and $p_{r,e}^{\mathrm{SpRS}}$ are accordingly expressed using the following equations:

$$p_{r,v}^{\mathrm{AC}} = p_{r,v}^{\mathrm{F,AC}} + p_{r,v}^{\mathrm{B,AC}} \quad (16)$$

$$p_{r,e}^{\mathrm{SpRS}} = p_{r,e}^{\mathrm{F,SpRS}} + p_{r,e}^{\mathrm{B,SpRS}} \quad (17)$$

where $p_{r,v}^{\mathrm{F,AC}}$ and $p_{r,v}^{\mathrm{B,AC}}$ denote the forward and backward photon leakage between adjacent wavelength channels, respectively. And $p_{r,e}^{\mathrm{SpRS}}$ includes the forward and backward SpRS, i.e., $p_{r,e}^{\mathrm{F,SpRS}}$ and $p_{r,e}^{\mathrm{B,SpRS}}$, respectively. Specifically, these values can be calculated with reference to [5].

The following constraints ensure routing validity:

$$\sum_{j\in V} K_{(i,j)}^{r} - \sum_{j\in V} K_{(j,i)}^{r} = \begin{cases} 1, & i = s_r \\ -1, & i = d_r \\ 0, & \text{otherwise} \end{cases} \quad \forall i \in V, \forall r \in R \quad (18)$$

$$0 < \sum_{v\in V} K_{v}^{r} \le |V|, \ \forall r \in R \quad (19)$$

$$0 < \sum_{e\in E} K_{e}^{r} \le |E|, \ \forall r \in R \quad (20)$$

$$0 \le \sum\nolimits_{\lambda_f \in W_e} K_{\lambda_f}^{r} \le |W| - 1, \ \forall r \in R \quad (21)$$

$$\sum\nolimits_{\lambda_{fm} \in W_e} K_{\lambda_{fm}}^{e} = 1, \ \forall e \in E \quad (22)$$

Equations (18–21) enforce routing constraints on traversed nodes and assigned wavelengths for each service r. Equation (22) ensures that each link hosts at most one QKD system. Based on the above formulation, we define a QP objective to maximize Φ_R under a service queue of R. Higher values of Φ_R indicate improved resource utilisation for data services and key generation with reduced quantum-classical interference. The objective function is thus formulated as:

$$\text{Maximize } \Phi_R = \sum_{r\in R}(\alpha \cdot \widehat{u_r^{\mathrm{C}}} - \delta \cdot \widehat{I_r^{\mathrm{CQ}}}) + \beta \cdot \widehat{u^{\mathrm{Q}}} \quad (23)$$

IV. Simulation Results

We consider three metropolitan network topologies (i.e., ring, tree, and mesh), as shown in Fig. 3, to validate the QP solutions. Each edge is set to 50 km in length, while secondary links in the tree topology are configured as 20 km to simulate access network conditions. The C-band accommodates 40 equally spaced wavelength channels at 0.8 nm intervals. The two-decoy-state BB84 protocol is adopted, with DV-QKD system parameters settled as shown in Table 1 [5]. The QCh orientation follows the ascending order of node indexes, from transmitter to receiver. The QP model was solved using IBM ILOG CPLEX v12.7.1 on a server with 128 GB of RAM.

TABLE I. Parameter Settings for the DV-QKD System

Parameter	Value
Average photon number per signal pulse, μ	0.48
Phase-distortion error probability, e_d	0.015
Quantum efficiency of detectors, η_{d}	0.3
Channel loss coefficient, α	0.2 dB/km
Dark count probability, p_{d}	1×10^{-7}
Pulse repetition frequency, f_s	1 GHz
Initial power of DCh, P^{1}	-18 dBm

The number of services ranges from 4 to 14 at an interval of 2, each with randomly selected source and destination nodes. The arrival time of the services queue follows a Poisson distribution. For the first-fit benchmark, the services queue is processed by sequence. In contrast, all service requests are input to the QP solver as a batch for joint optimisation. After each round of service provisioning, we calculate the network-wide average secret key rate (SKR) based on the accepted services. Figure 4 compares the network average SKR among the QP solutions and the first-fit benchmark. We adopt three sets of weighting factors (i.e., $[\alpha = 1, \delta = 0.01, \beta = 1]$, $[\alpha = 1, \delta = 1, \beta = 1]$, $[\alpha = 1, \delta = 100, \beta = 1]$), and two solver time constraints (i.e., 300 s and 900 s), forming six solutions for comparison. The weighting factors reflect the assigned relative weight of the interference term compared to resource utilisation in the objective function. These sets of weighting factors represent low, balanced, and high emphasis on interference, respectively.

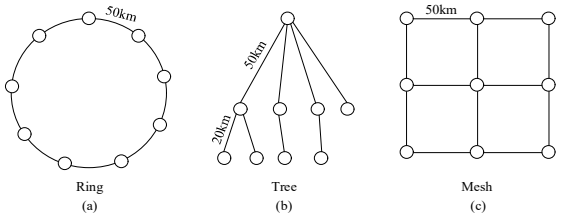

Fig. 3. 9-node (a) ring, (b) tree, and (c) mesh topologies.

In the ring network topology, the first-fit benchmark achieves an average SKR of 1.35 Mbit/s for 4 services, outperforming the QP solution with $[\alpha = 1, \delta = 0.01, \beta = 1]$. When δ is set to 100, the QP solution achieves a higher average SKR of 2.18 Mbit/s. As the number of service arrivals increases to 14, the QP solution achieves an average SKR of 0.19 Mbit/s, while the other solutions and the benchmark gradually decline to zero. In the ring topology, it can be observed that the solver time constraints have no obvious influence on the optimisation results. This can be attributed to the relatively fixed pattern of network connectivity. These results further suggest that increasing the interference weight leads to greater QKD capacity, which effectively preserves quantum signal integrity.

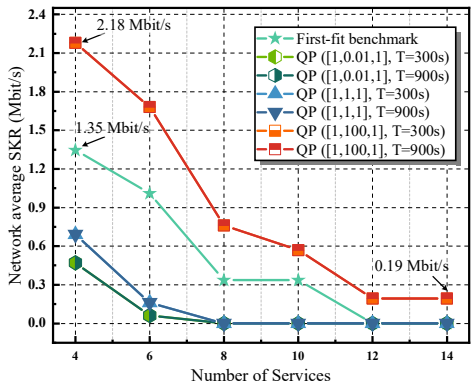

Fig. 4. Network average SKR comparison between first-fit benchmark and QP solutions in the ring topology.

As shown in Fig. 5, the first-fit benchmark maintains network average SKR at approximately 0.38 Mbit/s across 4 to 8 services in the tree topology. The SKR begins to degrade, reaching zero at 10 services. The QP solutions achieve

improvements across all service loads. The maximum SKR is achieved under $[\alpha = 1, \delta = 100, \beta = 1]$ as 6.51 Mbit/s. The other solutions under $[\alpha = 1, \delta = 0.01, \beta = 1]$ achieves a maximum SKR of 4.22 Mbit/s. It is noteworthy that, when δ is set as 1, the solution obtained with a longer solver time of 900 s clearly outperforms the 300 s counterpart, especially under higher service loads. At 14 services, the average SKR achieved by QP solutions are 1.91 Mbit/s and 4.82 Mbit/s, respectively, where the 900 s solution achieves a 152.4% improvement on average SKR. This demonstrates the benefit of extended solver time, particularly under high service loads. In the tree topology, it can be observed that the increasing value of δ still introduces better performance, while the first-fit benchmark leads to QKD service interruptions.

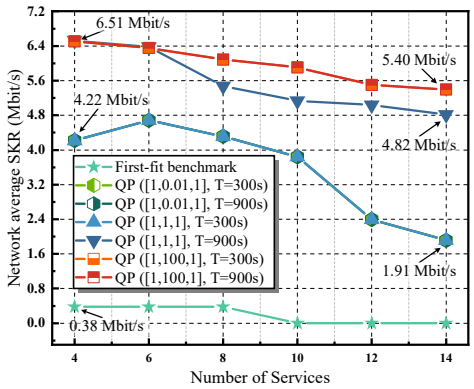

Fig. 5. Network average SKR comparison between first-fit benchmark and QP solutions in the tree topology.

As shown in Fig. 6, in the mesh topology, the first-fit benchmark achieves 1.01 Mbit/s and 0.50 Mbit/s under 4 and 6 services, respectively, which surpasses the QP solutions when δ is set as 0.01 and 1, where the highest SKR reaches 0.98 Mbit/s. Similar to the situations in ring and tree topologies, when δ is set as 100, the QP solution outperforms the benchmark, with SKR reaching 1.55 Mbit/s. Furthermore, for δ values of 0.01 and 100, extending the solver time from 300 s to 900 s yields improvements. At 14 services, for instance, the SKR with $\delta = 100$ increases from 0.72 Mbit/s to 0.75 Mbit/s. This result suggests that a moderate computation time increase can further achieve an improved network capacity. However, as the number of services increases to 10, both benchmark and other QP solutions drop to zero SKR. Meanwhile, comparing with the identical fibre-length ring topology, the mesh topology shows greater QKD capacity under light service loads.

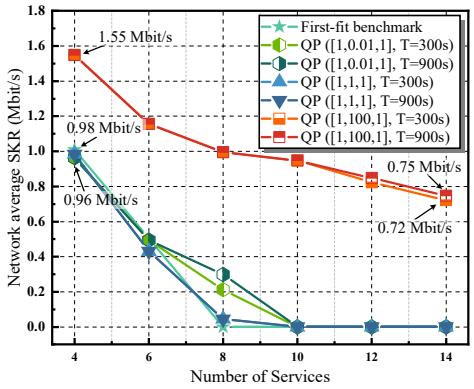

Fig. 6. Network average SKR comparison between first-fit benchmark and QP solutions in the mesh topology.

V. Conclusions

To support quantum-resistant encryption services, quantum key distribution (QKD) can be integrated into existing C-band optical networks. Instead of improving the system configuration, we identify a service provisioning perspective for network improvement. In this paper, we investigate a service provisioning optimisation method, which aims to maximise the network capacity for both QKD and data services. We formulate it as a quadratic programming model, where the classical-quantum network capacity is used as the optimisation objective. Simulation results show an increase in average secret key rate from 0.38 Mbit/s to 6.51 Mbit/s in a 9-node mesh topology, compared with the first-fit benchmark. The QKD service remains operational with up to 14 concurrently coexisting legacy data services.

Acknowledgment

This work was supported by NSFC project (62350001, 62425105, U22B2026), Quantum Science and Technology-National Science and Technology Major Project (2021ZD0300701), the Funds for Creative Research Groups of China (62021005), Fundamental Research Funds for BUPT (2025JCTP02), and BUPT Excellent Ph.D. Students Foundation (CX2023140). (Corresponding author: Xiaosong Yu and Yongli Zhao)

References

[1] Y. Cao *et al.*, "The evolution of quantum key distribution networks: On the road to the qinternet," IEEE Commun. Surv. Tut., vol. 24, no. 2, pp. 839–894, January 2022.

[2] X. Yu *et al.*, "Secret-Key Provisioning With Collaborative Routing in Partially-Trusted-Relay-based Quantum-Key-Distribution-Secured Optical Networks," J. Lightwave Technol., vol. 40, no. 12, pp. 3530–3545, February 2022.

[3] X. Yu *et al.*, "Multi-path-based quasi-real-time key provisioning in quantum-key-distribution enabled optical networks (QKD-ON)," Opt. Express, vol. 29, no. 14, pp. 21225–21239, July 2021.

[4] J. Li *et al.*, "Integration of Quantum Key Distribution Networks and Classical Networks: An Evolution Perspective," IEEE Network, vol. 39, no. 3, pp. 180–187, February 2025.

[5] S. Bahrani, M. Razavi, and J. A. Salehi, "Wavelength assignment in hybrid quantum-classical networks," Sci. Rep., vol. 8, no. 1, pp. 3456, February 2018.

[6] J. Wang, B. J. Rollick, Z. Jia, and B. A. Huberman, "Time-interleaved C-band Co-propagation of quantum and classical channels," J. Lightwave Technol., vol. 42, no. 11, pp. 4086–4095, June 2024.

[7] O. Alia *et al.*, "Bi-directional Coexistence of C-band Quantum Channel with Quantum-Safe IPsec DWDM Classical Channels in a Metropolitan Network," in Opt. Fiber Commun. Conf. Exhib., San Diego, California, USA, 2025, pp. Tu2D.4.

[8] V. V. Garbhapu, C. Ware, and M. Lourdiane, "Minimal impact network-wide heuristics for the coexistence of classical and CV-QKD signals in the C-band," in Eur. Conf. Opt. Commun., Frankfurt, Germany, 2024, pp. 1412–1415.

[9] L. Ruiz, and J. C. Garcia-Escartin, "Routing and wavelength assignment in hybrid networks with classical and quantum signals," IEEE J. Sel. Area Comm., vol. 43, no. 2, pp. 412–421, February 2025.

[10] Y. Liu, X. Yu, Y. Cao, A. Nag, and Y. Zhao, "Quantum-aware routing and wavelength assignment for classical traffic in hybrid quantum-classical optical networks," Opt. Express, vol. 33, no. 24, pp. 50519–50536, Nov. 2025.

[11] D. Gottesman, H. K. Lo, N. Lutkenhaus, and J. Preskill, "Security of quantum key distribution with imperfect devices," in IEEE Int Symp Inf Theor Proc, Chicago, Illinois, USA, 2004, pp. 136.